

## Observation of an emergent coherent state in the iron-based superconductor $\text{KFe}_2\text{As}_2$

Run Yang,<sup>1,2,3</sup> Zhiping Yin,<sup>4,\*</sup> Yilin Wang,<sup>2</sup> Yaomin Dai,<sup>2</sup> Hu Miao,<sup>2</sup> Bing Xu,<sup>1</sup>  
Xianggang Qiu,<sup>1,3,5,†</sup> and Christopher C. Homes<sup>2,‡</sup>

<sup>1</sup>Beijing National Laboratory for Condensed Matter Physics, Institute of Physics, Chinese Academy of Sciences, Beijing 100190, China

<sup>2</sup>Condensed Matter Physics and Materials Science Division, Brookhaven National Laboratory, Upton, New York 11973, USA

<sup>3</sup>School of Physical Sciences, University of Chinese Academy of Sciences, Beijing 100049, China

<sup>4</sup>Center for Advanced Quantum Studies and Department of Physics, Beijing Normal University, Beijing 100875, China

<sup>5</sup>Collaborative Innovation Center of Quantum Matter, Beijing 100084, China

(Received 1 August 2017; published 14 November 2017)

The *ab*-plane optical properties of  $\text{KFe}_2\text{As}_2$  single crystals have been measured over a wide temperature and frequency range. Below  $T^* \simeq 155$  K, where this material undergoes an incoherent-coherent crossover, a new coherent response emerges in the optical conductivity. A spectral weight analysis suggests that this feature originates from high-energy bound states. Below  $\simeq 75$  K the scattering rate for this feature is quadratic in temperature, indicating a Fermi-liquid response. Theoretical calculations suggest this crossover is dominated by the  $d_{xy}$  orbital. Our results indicate Kondo-type screening is the likely mechanism for the incoherent-coherent crossover in hole-overdoped  $\text{KFe}_2\text{As}_2$ .

DOI: 10.1103/PhysRevB.96.201108

Investigating the role of electronic correlations in systems with large orbital degrees of freedom remains a key challenge in understanding the multiorbital physics in iron-based superconductors (FeSCs) [1–7]. Previous studies found that, due to Hund's coupling, the electron correlations depend strongly on the band filling and are responsible for the electron-hole asymmetry in FeSCs [8,9]. Electron doping weakens the correlations and eventually yields Fermi-liquid (FL) behavior [10,11], while hole doping increases the correlations [12] due to strong Hund's rule coupling and the proximity to half filling [9].  $\text{KFe}_2\text{As}_2$ , an extremely hole-doped FeSC, is expected to be strongly correlated with non-FL behavior [2]. A bad metal at room temperature, carriers start to form coherent quasiparticles below  $T^* \simeq 155$  K, and most strikingly, a FL state with  $T^2$  resistivity is observed up to 75 K [13–15]. These results have prompted an extensive debate about the driving mechanism between orbital-selective Mottness, in which the intraorbital Coulomb interaction plays the dominant role and drives the strong localization of a selected orbital at higher temperatures ( $\gtrsim 150$  K), and the Kondo-type screening of local spins which is driven by interorbital Hund's rule coupling [16–19].

In this Rapid Communication we examine the temperature dependence of the optical conductivity of  $\text{KFe}_2\text{As}_2$  to investigate the nature of the incoherent-coherent crossover. As the temperature is lowered across  $T^*$ , spectral weight is transferred from high ( $\simeq 2000$ – $3000$   $\text{cm}^{-1}$ ) to low energy ( $\lesssim 1000$   $\text{cm}^{-1}$ ) into a new emergent Drude peak, which displays a FL behavior below  $\simeq 75$  K. To further investigate this behavior, we performed dynamical mean-field theory (DMFT) calculations that suggest that the incoherent-coherent crossover is governed by the  $d_{xy}$  orbital. The FL behavior indicates a Kondo-type screening of local spin moments, which is consistent with susceptibility [14] and transport measurements [20], and in agreement with the theoretical prediction [19,21]. However, the absence of a Mott gap in

the high-temperature optical spectra does not agree with the scenario of orbital-selective Mottness. We propose that Kondo-type screening is the mechanism responsible for the orbital-selective incoherent-coherent crossover in  $\text{KFe}_2\text{As}_2$ , which is close to half filling. This result introduces constraints on theoretical investigations of the orbital physics in correlated materials as well as the pairing mechanism in the FeSCs.

High-quality single crystals of  $\text{KFe}_2\text{As}_2$  with good cleavage planes (001) were synthesized using the self-flux method [22]. The reflectance from freshly cleaved surfaces has been measured over a wide temperature ( $\sim 5$ – $300$  K) and frequency range ( $\sim 2$  meV to about 5 eV) at a near-normal angle of incidence for light polarized in the *ab* planes using an *in situ* evaporation technique [23]. The optical conductivity has been determined from a Kramers-Kronig analysis of the reflectivity (the reflectivity and the details of the Kramers-Kronig analysis may be found in the Supplemental Material [24]).

The temperature dependence of the optical conductivity  $\sigma_1(\omega)$  is shown in Fig. 1 in the infrared region. The free-carrier response is typically a Lorentzian centered at zero frequency where the width at half maximum is the scattering rate. At high temperature, the conductivity is low and resembles a bad metal; the nearly flat frequency response indicates a large scattering rate, signaling an almost incoherent response. As the temperature is reduced, the low-frequency conductivity increases gradually until 150 K, at which point a new Drude-like peak appears superimposed on the broad response, resulting in a kink in the low-energy conductivity (denoted by the arrow in Fig. 1, as well as the sudden change in slope in the inset). This peak increases dramatically in strength and narrows quickly with decreasing temperature, reflecting its small scattering rate and coherent character [25].

Because of the multiband nature of FeSCs there is typically more than one type of free carrier present, so we employ a Drude-Lorentz model with multiple Drude components. The real part of the optical conductivity is

$$\sigma_1(\omega) = \frac{2\pi}{Z_0} \left[ \sum_j \frac{\omega_{p,j}^2 \tau_j}{(1 + \omega^2 \tau_j^2)} + \sum_k \frac{\gamma_k \omega^2 \Omega_k^2}{(\omega_k^2 - \omega^2)^2 + \gamma_k^2 \omega^2} \right],$$

\*yinzhiping@bnu.edu.cn

†xgqiu@iphy.ac.cn

‡homes@bnl.gov

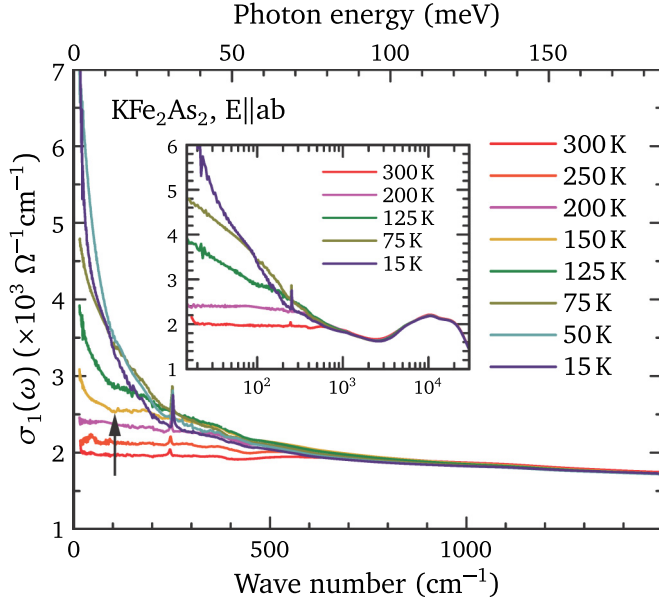


FIG. 1. The temperature dependence of the real part of the optical conductivity of  $\text{KFe}_2\text{As}_2$  above and below the incoherent-coherent crossover  $T^*$ . Inset: The optical conductivity at several temperatures over a broad frequency range.

where  $Z_0 \simeq 377 \Omega$  is the impedance of free space. The first term describes a sum of free-carrier Drude responses with plasma frequencies  $\omega_{p,j}^2 = 4\pi n_j e^2 / m_j^*$  ( $n_j$  represents the carrier concentration and  $m_j^*$  the effective mass), and scattering rates  $1/\tau_j$ . The second term is a sum of Lorentz oscillators with position  $\omega_k$ , width  $\gamma_k$ , and strength  $\Omega_k$ . At high temperature ( $T > 150 \text{ K}$ ), the real and imaginary parts of the optical conductivity are fit simultaneously and are described quite well by two Drude components and two Lorentz terms [Fig. S2(a) of the Supplementary Material]: a narrow Drude (D1) with a  $T$ -dependent scattering rate, and a broad Drude (D2), which is almost  $T$  independent, indicating two groups of carriers [26,27]. The narrow Drude reflects the coherent response and the broad Drude corresponds to the incoherent background. Below 150 K, the newly formed peak and corresponding kink in  $\sigma_1(\omega)$  makes it difficult to fit the low-energy response with only two Drude components, so a third Drude component (D3) has been introduced. The existence of a new Drude component can also be realized by fitting the reflectivity and the imaginary part of the optical conductivity (Table I and Figs. S2 and S3 in the Supplemental Material).

Below  $T^*$  the complex conductivity is described quite well using three Drude and two Lorentz components; the result for  $\sigma_1(\omega)$  at 125 K is shown in Fig. 2(a). The temperature dependences of the Drude components are summarized in Figs. 2(b)–2(e). As the temperature is reduced, the values for  $\omega_p$  for the narrow and broad Drude terms, D1 and D2, respectively, remain essentially constant. Below  $T^*$  the plasma frequency for the newly developed Drude component (D3) increases steadily and  $\omega_{p,D3}^2(T)$  follows a mean-field temperature dependence [Fig. S4(a) in the Supplemental Material]. Figures 2(d) and 2(e) show the temperature dependence of the scattering rates;  $1/\tau_{D2}$  is almost temperature independent, while  $1/\tau_{D1} \propto T$ . Below  $T^*$ , there is some initial uncertainty

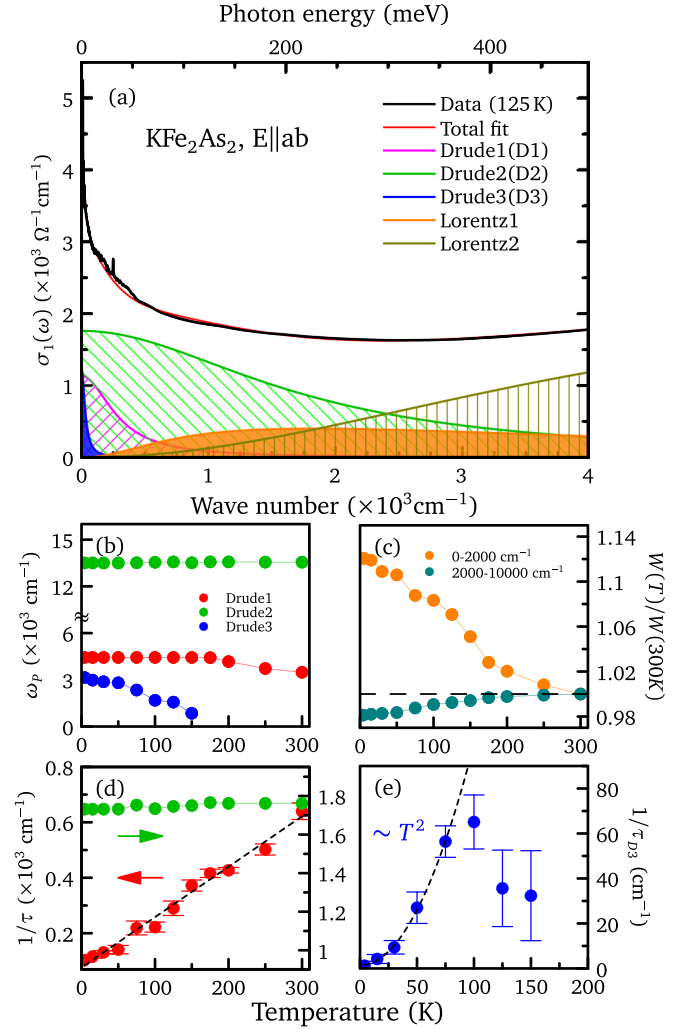


FIG. 2. (a) Fit of the Drude-Lorentz model to the  $\sigma_1(\omega)$  of  $\text{KFe}_2\text{As}_2$  at 125 K, decomposed into individual Drude and Lorentz terms. (b) The plasma frequency  $\omega_p$  for the three Drude components. (c) Temperature dependence of the spectral weight  $W(\omega_1, \omega_2, T)$  for various lower and upper cutoff frequencies. (d) Scattering rates for the narrow Drude (D1) (red) and broad Drude (D2) (green) components are extracted from the fits. The dashed line is the linear fit to  $1/\tau_{D1}$ . (e) The scattering rate of the emergent Drude component. The dashed line is the quadratic fit to  $1/\tau_{D3}$  below 75 K.

regarding the behavior of  $1/\tau_{D3}$ , but for  $T < T_{FL}$ , FL behavior is observed,  $1/\tau_{D3} \propto T^2$ .

In order to understand the origin of the new peak (D3), we calculated the spectral weight of  $\sigma_1(\omega)$ ,

$$W(\omega_1, \omega_2, T) = \int_{\omega_1}^{\omega_2} \sigma_1(\omega, T) d\omega,$$

over different frequency intervals and normalized the result to the room-temperature value. In Fig. 2(c), below 150 K, the spectral weight between  $\sim 0$  and  $2000 \text{ cm}^{-1}$  is greatly enhanced, while the spectral weight in the high-energy region ( $2000\text{--}10\,000 \text{ cm}^{-1}$ ) is depleted. We note that while  $\omega_{p,D1}$  and  $\omega_{p,D2}$  are temperature independent below 150 K, the overall spectral weight up to  $10\,000 \text{ cm}^{-1}$  remains constant [Fig. S4(b) in the Supplemental Material] (the optical conductivity above

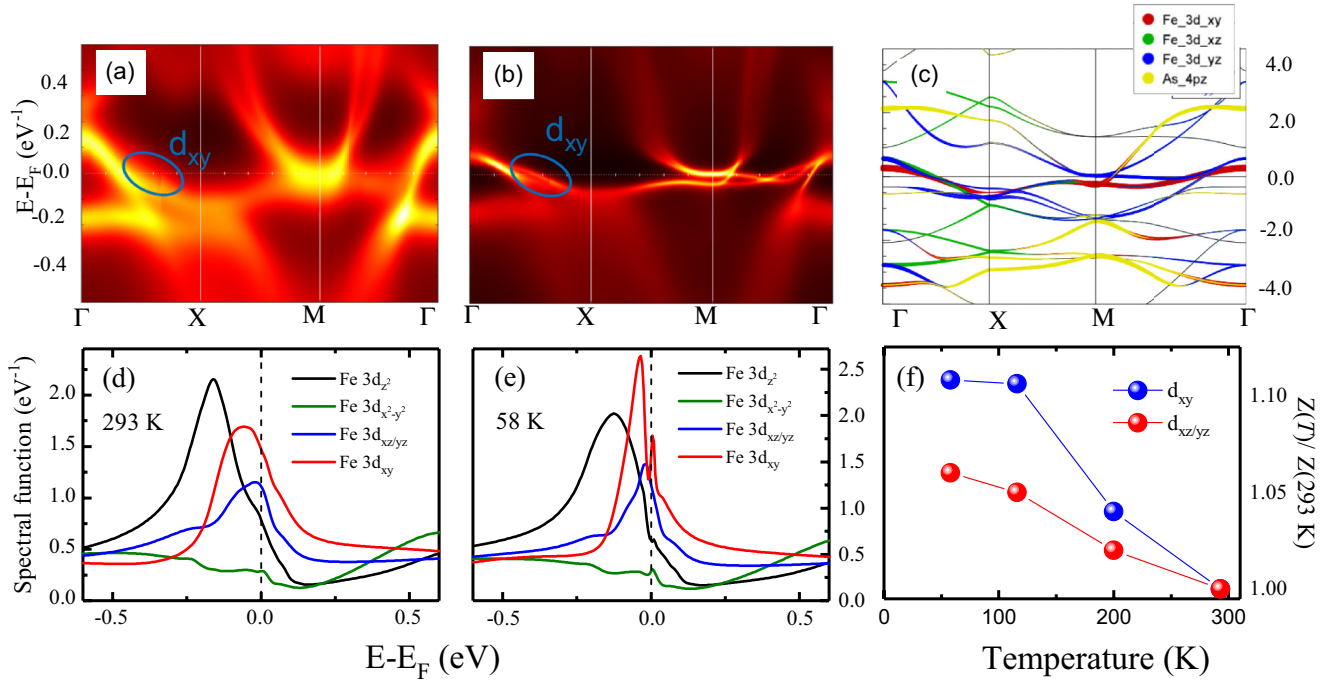


FIG. 3. The electronic structure of  $\text{KFe}_2\text{As}_2$  above and below the incoherent-coherent crossover. (a) DFT+DMFT band structure for  $\text{KFe}_2\text{As}_2$  at 293 K and (b) 58 K; the blue ellipses denote the band of primarily  $d_{xy}$  character. (c) DFT band structure. (d) The Fe- $d$  orbital character for the density of states of  $\text{KFe}_2\text{As}_2$  at 293 K and (e) 58 K. (f) The temperature-dependent quasiparticle spectral weight  $Z$  calculated by integrating the spectral function near  $E_F$ .

$10\,000\text{ cm}^{-1}$  does not vary with temperature). We propose that the new Drude component emerges out of a high-energy bound state above  $2000\text{ cm}^{-1}$  ( $\sim 0.25\text{ eV}$ ), which originates from the small overlap between the local spin-polarized atomic states and the single-particle states driven by the Hund's coupling, indicating that some incoherent bands start to form coherent quasiparticles with an underlying Fermi surface, which is the typical signature for the incoherent-coherent crossover [19,28]. Previous angle-resolved photoemission spectroscopy (ARPES) measurements [18,29] observed a slight decrease of the spectral weight of a band near the Fermi level with increasing temperature. Here, we offer clear evidence of spectral weight transfer during this process in a system that is close to half filling.

Because D3's intensity is significantly enhanced and becomes very sharp at low temperatures, it dominates the dc conductivity below 75 K [Fig. S2(b) in the Supplemental Material]; its  $T^2$ -dependent scattering rate, indicating FL behavior [30], is in agreement with recent transport measurements [20]. The extremely low scattering rate for D3 reflects the high quality of these samples ( $\text{RRR} \sim 512$ ); however, the presence of disorder might explain the absence of FL behavior observed in another study [31]. The existence of two different kinds of narrow Drude components points to strong orbital differentiation in FeSCs [9,14].

To better understand the origin of the emergent Drude component, calculations for  $\text{KFe}_2\text{As}_2$  were performed using density functional theory (DFT), and extended using dynamical mean-field theory (DMFT) (the details of which are described in the Supplemental Material); DFT+DMFT has been shown to accurately reproduce the electronic behavior of

strongly correlated materials where DFT alone typically fails [2,32,33]. The results are summarized in Fig. 3. Consistent with ARPES [34,35] and de Haas-van Alphen oscillation measurements [36], only hole-like Fermi surfaces are present in  $\text{KFe}_2\text{As}_2$ . From the temperature-dependent band structure, we note that at high temperature [293 K, Fig. 3(a)], the band with  $d_{xy}$  orbital character is much less pronounced than those dominated by the  $d_{xz/yz}$  orbitals. However, at low temperature [58 K, Fig. 3(b)], the  $d_{xy}$  character increases dramatically. These changes are reflected in the temperature dependence of the density of states (DOS) for different orbital characters [Fig. 3(d) at 293 K, and Fig. 3(e) at 58 K], where the  $d_{xy}$  DOS sharpens at low temperature and dominates the low-energy DOS, signaling an incoherent-coherent crossover. This suggests that the emergent coherent peak in the optical conductivity below 150 K is most likely dominated by the  $d_{xy}$  orbital.

In most iron-based superconductors, the state near  $E_F$  arises mainly from the  $t_{2g}$  orbitals; correlation effects will give rise to charge transfer from the  $d_{xy}$  to  $d_{xz/yz}$  orbitals [37,38]. Comparing the DFT+DMFT band structure in Fig. 3(b) with that of DFT in 3(c) [also see Fig. S5(b) in the Supplemental Material], the presence of electronic correlations leads to an increase in the contribution of the  $d_{xy}$  band to the Fermi surface, while the  $d_{xz/yz}$  contribution decreases in order to maintain the Luttinger count. In this hole-overdoped system ( $5.5e/\text{Fe}$ ), charge transfer pushes the  $d_{xy}$  orbital much closer to half filling [8], and Hund's rule coupling results in a strong renormalization of this orbital [8,9], with the renormalization factor  $1/Z \propto U/t$ , where  $t$  is the hybridization magnitude and  $Z$  is the quasiparticle spectral weight. Thus, at high

temperature, the  $d_{xy}$  orbital is more incoherent (localized) and contributes to the local moment, resulting in a Curie-Weiss susceptibility [14]. At low temperature, the quasiparticle spectral weight (proportional to the hybridization of  $d_{xy}$  orbital between nearest-neighbor atoms), is enhanced continuously [39] [Fig. 3(f)]. Below 150 K, this orbital begins to delocalize and form coherent quasiparticles, which is consistent with the observation of spectral weight transfer from the high-to low-energy region and the formation of a new coherent peak in the optical conductivity [Fig. 2(c)]. Below 75 K, FL behavior ( $1/\tau_{D3} \propto T^2$ ) is observed. This result, combined with the Pauli-like susceptibility [14], indicates Kondo-type screening, during which the local moments are totally screened by the conduction electrons, resulting in a saturated spin susceptibility and diminished scattering from local spins [19]. Furthermore, we find that at 58 K, the inverse lifetime ( $\hbar/\tau$ ) on the  $d_{xy}$  orbital is about 1 meV which is smaller than  $k_B T \simeq 5.8$  meV, while  $\hbar/\tau$  on the  $d_{xz/yz}$  orbital is 7 meV. Thus, at low temperature, the well-defined quasiparticles are mainly on  $d_{xy}$ . In our results, we also note that  $\hbar/\tau_{D3} < k_B T < \hbar/\tau_{D1}$ , indicating that the newly formed Drude component and the FL behavior below 75 K is dominated by the  $d_{xy}$  orbital.

The absence of this behavior in a simple DFT calculation indicates that this incoherent-coherent crossover is the result of electronic correlations driven by Hund's rule coupling [15,16] (Fig. S5 in the Supplemental Material). While the spectral weight in the optical conductivity is transferred from a low-to high-energy region upon warming, the absence of a gaplike structure in the optical conductivity and the residual DOS of the  $d_{xy}$  orbital near the Fermi level at 293 K are inconsistent with the description of an orbital-selective Mott transition [40]; instead, our observation argues for an orbital-selective incoherent-coherent crossover in a Hund's metal [19,41,42].

In summary, we have observed an emergent Drude peak in the optical conductivity of  $\text{KFe}_2\text{As}_2$  associated with the incoherent-coherent crossover below  $T^* \simeq 155$  K, and determined that it originates from a high-energy bound state. Below 75 K, this response sharpens quickly and shows FL behavior, which may come from Kondo-type screening by the delocalized electrons. Based on DFT+DMFT calculations, we find that this new peak is dominated by the  $d_{xy}$  orbital, reflecting an orbital-selective incoherent-coherent crossover. We propose that in  $\text{KFe}_2\text{As}_2$ , which is close to half filling, the incoherent-coherent crossover is related to the Hund's rule driven Kondo-type screening, rather than orbital-selective Mottness.

We thank I. Zaliznyak, A. Wang, and W. Yin for useful discussions. Work at the Chinese Academy of Science was supported by NSFC (Projects No. 11374345 and No. 91421304) and MOST (Projects No. 2015CB921303 and No. 2015CB921102). Work at Beijing Normal University was supported by the National Natural Science Foundation of China (Grant No. 11674030) and the National Key Research and Development Program of China (Contract No. 2016YFA0302300). Work at Brookhaven National Laboratory was supported by the Office of Science, US Department of Energy under Contract No. DE-SC0012704. H.M. was supported by the Center for Emergent Superconductivity, an Energy Frontier Research Center funded by the US DOE, Office of Basic Energy Sciences. Y.L.W. was supported by the US Department of energy, Office of Science, Basic Energy Sciences as a part of the Computational Materials Science Program through the Center for Computational Design of Functional Strongly Correlated Materials and Theoretical Spectroscopy.

- 
- [1] P. Richard, T. Sato, K. Nakayama, S. Souma, T. Takahashi, Y.-M. Xu, G. F. Chen, J. L. Luo, N. L. Wang, and H. Ding, *Phys. Rev. Lett.* **102**, 047003 (2009).
- [2] Z. P. Yin, K. Haule, and G. Kotliar, *Nat. Mater.* **10**, 932 (2011).
- [3] M. M. Qazilbash, J. J. Hamlin, R. E. Baumbach, L. Zhang, D. J. Singh, M. B. Maple, and D. N. Basov, *Nat. Phys.* **5**, 647 (2009).
- [4] A. Georges, L. de' Medici, and J. Mravlje, *Annu. Rev. Condens. Matter Phys.* **4**, 137 (2013).
- [5] R. Yu and Q. Si, *Phys. Rev. B* **84**, 235115 (2011).
- [6] D. H. Lu, M. Yi, S.-K. Mo, A. S. Erickson, J. Analytis, J.-H. Chu, D. J. Singh, Z. Hussain, T. H. Geballe, I. R. Fisher, and Z.-X. Shen, *Nature (London)* **455**, 81 (2008).
- [7] X. Chen, P. Dai, D. Feng, T. Xiang, and F.-C. Zhang, *Nat. Sci. Rev.* **1**, 371 (2014).
- [8] L. de Medici, G. Giovannetti, and M. Capone, *Phys. Rev. Lett.* **112**, 177001 (2014).
- [9] L. de Medici, J. Mravlje, and A. Georges, *Phys. Rev. Lett.* **107**, 256401 (2011).
- [10] F. L. Ning, K. Ahilan, T. Imai, A. S. Sefat, M. A. McGuire, B. C. Sales, D. Mandrus, P. Cheng, B. Shen, and H.-H. Wen, *Phys. Rev. Lett.* **104**, 037001 (2010).
- [11] P. Werner, M. Casula, T. Miyake, F. Aryasetiawan, A. J. Millis, and S. Biermann, *Nat. Phys.* **8**, 331 (2012).
- [12] F. Hardy, A. E. Böhmer, L. de' Medici, M. Capone, G. Giovannetti, R. Eder, L. Wang, M. He, T. Wolf, P. Schweiss, R. Heid, A. Herbig, P. Adelman, R. A. Fisher, and C. Meingast, *Phys. Rev. B* **94**, 205113 (2016).
- [13] F. Eilers, K. Grube, D. A. Zocco, T. Wolf, M. Merz, P. Schweiss, R. Heid, R. Eder, R. Yu, J.-X. Zhu, Q. Si, T. Shibauchi, and H. v. Löhneysen, *Phys. Rev. Lett.* **116**, 237003 (2016).
- [14] F. Hardy, A. E. Böhmer, D. Aoki, P. Burger, T. Wolf, P. Schweiss, R. Heid, P. Adelman, Y. X. Yao, G. Kotliar, J. Schmalian, and C. Meingast, *Phys. Rev. Lett.* **111**, 027002 (2013).
- [15] K. Haule and G. Kotliar, *New J. Phys.* **11**, 025021 (2009).
- [16] L. Fanfarillo and E. Bascones, *Phys. Rev. B* **92**, 075136 (2015).
- [17] S. Backes, H. O. Jeschke, and R. Valentí, *Phys. Rev. B* **92**, 195128 (2015).
- [18] H. Miao, Z. P. Yin, S. F. Wu, J. M. Li, J. Ma, B.-Q. Lv, X. P. Wang, T. Qian, P. Richard, L.-Y. Xing, X.-C. Wang, C. Q. Jin, K. Haule, G. Kotliar, and H. Ding, *Phys. Rev. B* **94**, 201109 (2016).
- [19] K. M. Stadler, Z. P. Yin, J. von Delft, G. Kotliar, and A. Weichselbaum, *Phys. Rev. Lett.* **115**, 136401 (2015).
- [20] Z. J. Xiang, N. Z. Wang, A. F. Wang, D. Zhao, Z. L. Sun, X. G. Luo, T. Wu, and X. H. Chen, *J. Phys.: Condens. Matter* **28**, 425702 (2016).

- [21] C. Aron and G. Kotliar, *Phys. Rev. B* **91**, 041110 (2015).
- [22] J. S. Kim, E. G. Kim, G. R. Stewart, X. H. Chen, and X. F. Wang, *Phys. Rev. B* **83**, 172502 (2011).
- [23] C. C. Homes, M. Reedyk, D. A. Crandles, and T. Timusk, *Appl. Opt.* **32**, 2976 (1993).
- [24] See Supplemental Material <http://link.aps.org/supplemental/10.1103/PhysRevB.96.201108> for details of sample growth and characterization, reflectance and Kramers-Kronig analysis, fits to the complex conductivity, spectral weight analysis, and electronic structure calculations, which includes Refs. [43,44,45].
- [25] Y. M. Dai, A. Akrap, J. Schneeloch, R. D. Zhong, T. S. Liu, G. D. Gu, Q. Li, and C. C. Homes, *Phys. Rev. B* **90**, 121114 (2014).
- [26] D. Wu, N. Barišić, P. Kallina, A. Faridian, B. Gorshunov, N. Drichko, L. J. Li, X. Lin, G. H. Cao, Z. A. Xu, N. L. Wang, and M. Dressel, *Phys. Rev. B* **81**, 100512 (2010).
- [27] Y. M. Dai, B. Xu, B. Shen, H. Xiao, H. H. Wen, X. G. Qiu, C. C. Homes, and R. P. S. M. Lobo, *Phys. Rev. Lett.* **111**, 117001 (2013).
- [28] K. Takenaka, R. Shiozaki, S. Okuyama, J. Nohara, A. Osuka, Y. Takayanagi, and S. Sugai, *Phys. Rev. B* **65**, 092405 (2002).
- [29] M. Yi, Z.-K. Liu, Y. Zhang, R. Yu, J.-X. Zhu, J. Lee, R. Moore, F. Schmitt, W. Li, S. Riggs, J.-H. Chu, B. Lv, J. Hu, M. Hashimoto, S.-K. Mo, Z. Hussain, Z. Mao, C. Chu, I. Fisher, Q. Si, Z.-X. Shen, and D. Lu, *Nat. Commun.* **6**, 7777 (2015).
- [30] Y. M. Dai, H. Miao, L. Y. Xing, X. C. Wang, P. S. Wang, H. Xiao, T. Qian, P. Richard, X. G. Qiu, W. Yu, C. Q. Jin, Z. Wang, P. D. Johnson, C. C. Homes, and H. Ding, *Phys. Rev. X* **5**, 031035 (2015).
- [31] J. K. Dong, S. Y. Zhou, T. Y. Guan, H. Zhang, Y. F. Dai, X. Qiu, X. F. Wang, Y. He, X. H. Chen, and S. Y. Li, *Phys. Rev. Lett.* **104**, 087005 (2010).
- [32] K. Haule, C.-H. Yee, and K. Kim, *Phys. Rev. B* **81**, 195107 (2010).
- [33] Z. P. Yin, K. Haule, and G. Kotliar, *Nat. Phys.* **7**, 294 (2011).
- [34] T. Yoshida, S.-i. Ideta, I. Nishi, A. Fujimori, M. Yi, R. Moore, S.-K. Mo, D. Lu, Z.-X. Shen, Z. Hussain, K. Kihou, C. H. Lee, A. Iyo, H. Eisaki, and H. Harima, *Front. Phys.* **2**, 17 (2014).
- [35] T. Sato, K. Nakayama, Y. Sekiba, P. Richard, Y.-M. Xu, S. Souma, T. Takahashi, G. F. Chen, J. L. Luo, N. L. Wang, and H. Ding, *Phys. Rev. Lett.* **103**, 047002 (2009).
- [36] T. Terashima, N. Kurita, M. Kimata, M. Tomita, S. Tsuchiya, M. Imai, A. Sato, K. Kihou, C.-H. Lee, H. Kito, H. Eisaki, A. Iyo, T. Saito, H. Fukazawa, Y. Kohori, H. Harima, and S. Uji, *Phys. Rev. B* **87**, 224512 (2013).
- [37] G. Lee, H. S. Ji, Y. Kim, C. Kim, K. Haule, G. Kotliar, B. Lee, S. Khim, K. H. Kim, K. S. Kim, K.-S. Kim, and J. H. Shim, *Phys. Rev. Lett.* **109**, 177001 (2012).
- [38] Y. Li, Z. Yin, X. Wang, D. W. Tam, D. L. Abernathy, A. Podlesnyak, C. Zhang, M. Wang, L. Xing, C. Jin, K. Haule, G. Kotliar, T. A. Maier, and P. Dai, *Phys. Rev. Lett.* **116**, 247001 (2016).
- [39] D. Fobes, I. A. Zaliznyak, Z. Xu, R. Zhong, G. Gu, J. M. Tranquada, L. Harriger, D. Singh, V. O. Garlea, M. Lumsden, and B. Winn, *Phys. Rev. Lett.* **112**, 187202 (2014).
- [40] M. M. Qazilbash, M. Brehm, B.-G. Chae, P.-C. Ho, G. O. Andreev, B.-J. Kim, S. J. Yun, A. V. Balatsky, M. B. Maple, F. Keilmann, H.-T. Kim, and D. N. Basov, *Science* **318**, 1750 (2007).
- [41] Z. P. Yin, K. Haule, and G. Kotliar, *Phys. Rev. B* **86**, 195141 (2012).
- [42] J. Mravlje, M. Aichhorn, T. Miyake, K. Haule, G. Kotliar, and A. Georges, *Phys. Rev. Lett.* **106**, 096401 (2011).
- [43] M. Dressel and G. Grüner, *Electrodynamics of Solids* (Cambridge University Press, Cambridge, UK, 2001).
- [44] F. Wooten, *Optical Properties of Solids* (Academic, New York, 1972), pp. 244–250.
- [45] N. L. Wang, W. Z. Hu, Z. G. Chen, R. H. Yuan, G. Li, G. F. Chen, and T. Xiang, *J. Phys.: Condens. Matter* **24**, 294202 (2012).